Charge Scheduling of Electric Vehicles in Smart Parking-Lot Under Future Demands Uncertainty

Omid Fallah-Mehrjardi, Mohammad Hossein Yaghmaee, *Senior Member, IEEE*, and Alberto Leon-Garcia, *Life Fellow, IEEE*

***Abstract*—In this study, a public parking-lot is assumed to schedule the charging of Electric Vehicles (EVs). Each EV owner upon arriving gives the energy demand as well as departure time to the system and immediately receives feedback; fulfilling or adjusting the request. The system designed in this study decides based on the previously admitted requests and the uncertain future demands in both Admission Control (AC) and Charge Scheduling (CS) mechanisms. We formulate a multi-stage stochastic programming model to minimize the expected total energy costs over the finite time horizon. Next, we approximate the model using a finite scenario tree. However, this model is computationally intractable, even for a moderate number of stages. Therefore, we customize a well-known decomposition procedure, Stochastic Dual Dynamic Programming (SDDP), to be matched the time-dependent charging conditions. Since the procedure takes several hours to obtain a high-quality solution, we run it once in the offline mode and employing the results for the online mode. The simulation results indicate that the proposed method outperforms the myopic approach, and obtains a close solution to the theoretical optimal value in terms of total costs and rejected demands.**

***Index Terms*—Electric vehicle, admission control, parking lot, decomposition, stochastic dual dynamic programming, multi-stage stochastic optimization, demand uncertainty.**

NOTATION

$\mathcal{T}$	Set of time slots indexed by $t = 1, \ldots, T$
$\mathcal{T}'$	Set of all time slots except the first
$\mathcal{T}_u$	Set of time horizon of user u
$\mathcal{S}$	Set of stages indexed by $s = 1, \ldots, S$
$\mathcal{T}^s$	Set of time slots after sth stage
U	Set of users (EVs) indexed by u
$U_{[t]}$	Set of existing users in the system up to t
$U^{s,j}$	Set of users at jth node of stage s
$\mathcal{X}_t$	Set of feasible decisions at time t
$\mathcal{X}^{s,j}$	Set of feasible decisions at jth node of stage s
$\mathcal{K}^s$	Set of generated cuts at stage s indexed by k
Ξ_t	Set of random data at time t indexed by ξ_t
$\xi_{[t]}$	History of random data realization up to t
$\xi^{s,j}$	Random data realization at jth node of stage s
a_u, d_u	User u's arrival and departure time
e_u	User u's energy demand
E^{max}	Max transformer capacity per time slot
x_u^{max}	Max charging rate of EV u per time slot
c_t	Predicted grid energy price per unit at time t
c^p	Penalty rate of rejected demands per unit at time t
$\mathfrak{c}_t, \mathfrak{c}^s$	Price symbol of total cost at time t, stage s
N^s	Number of nodes in the scenario tree at stage s
N	Total number of scenarios in the scenario tree
M	Number of selected scenarios for the forward pass
$\underline{z}, \bar{z}$	Lower and upper bound of objective function
$\bar{z}_h, \bar{z}_{avg}$	High and average values of statistical upper bound
$x_{u,t}$	Charging power allocation for user u at time t
$X_{u,t}$	Total allocated energy for user u up to time t
X_t^s	Total allocated energy at stage s up to time t
π_t	Dual variable associated with transformer capacity
ρ_k	Dual variable associated with generated cuts
$\underline{\pi}_t, \underline{\rho}_k$	Values of dual variables
$Q^{s,j}(\cdot)$	Total cost function at jth node of stage s
$\underline{Q}^{s,j}(\cdot)$	Value of total cost function
$\overline{Q}^s(\cdot)$	The recourse function at stage s
α^s	Constant coefficient of cuts at stage s
β_t^s	Variable coefficient of cuts at stage s at time t
$\sim$	is used above symbols to show the original symbol approximated by the Monte-Carlo sampling.

Manuscript received August 8, 2019; revised December 1, 2019 and May 10, 2020; accepted June 1, 2020. Date of publication June 9, 2020; date of current version October 21, 2020. Paper no. TSG-01158-2019. *(Corresponding author: Mohammad Hossein Yaghmaee.)*

Omid Fallah-Mehrjardi and Mohammad Hossein Yaghmaee are with the Department of Computer Engineering, Ferdowsi University of Mashhad, Mashhad 91779, Iran (e-mail: fallah@mail.um.ac.ir; hyaghmae@um.ac.ir).

Alberto Leon-Garcia is with the Department of Electrical and Computer Engineering, University of Toronto, Toronto, ON M5S 3G4, Canada (e-mail: alberto.leongarcia@utoronto.ca).

Color versions of one or more of the figures in this article are available online at http://ieeexplore.ieee.org.

Digital Object Identifier 10.1109/TSG.2020.3000850

I. INTRODUCTION

ELECTRIC vehicles play an essential role in reducing carbon emissions and preventing air pollution compared to traditional gasoline vehicles. The statistics show that one million plug-in EVs have been sold in the United States since Oct. 2018. This number has risen from below 5000 per month until Sep. 2012 to more than 20000 per month since May 2018 [1]. The dramatic growth of EVs in recent years, as well as the anticipation of the increasing trend in the decade ahead, is a great challenge for the smart grid. However, this load can be shifted to an appropriate time to decrease the pressure to the grid [2]. For example in uncontrolled charging conditions, almost 30% of network facilities need to be upgraded for an

EV penetration of 25%, while this can reduces to 5% if the load can be shifted to the off-peak periods [3].

One of the most appealing ways from views of both EV owner and the grid is charging the EVs in a parking-lot equipped with charging stations. This way provides flexibility to the grid as well as exploiting the EV idle time because the users usually stay in parking-lot longer than the charging time. Note that the day-time charging faces dynamic arrival and departure of the EVs and highly fluctuated electricity prices. Compared to the night-time parking-lot for residential buildings, those near commercial places create more attractive situations during day-time. Therefore, these types of parking lots have attracted much attention in the literature [3].

The literature related to optimal scheduling of the EVs in parking-lot is developing rapidly. Tabari and Yazdani [4] offer two options; fast or optimal charging, upon arriving the EV owner to parking-lot. Next, the system resolves deterministic linear programming for the AC or the CS problems whenever a new request comes. Moreover, Jiang and Zhen [5] integrate energy storage and photovoltaic systems with parking-lot that charge the arriving EVs based on a meta-heuristic algorithm.

Furthermore, several studies are devoted to pricing and charging of the users via the game-theoretical approach. First, Zhang and Li [6] propose a non-cooperative game in which each player (user) aims at maximizing the utility based on his/her demand, electricity price, and the available transformer capacity. Additionally, in research [7], the system offers menu-based pricing to a user based on different energy levels and deadline. Next, the game between the system and the user is modeled, whether the system knows the users' utility or not. More recently, Alinia *et al.* [8] design a game that the best strategy for the players (users) is truthfulness regardless of the others' behavior. In this case, the user says the true demand, and the system admits it with offering price according to social welfare maximization. In a similar study [9], a combinatorial auction is proposed to offer a pricing mechanism in order to maximize the social welfare. The future demand is also heuristically considered based on the past requests, not the future behavior forecast.

However, the above-mentioned studies [4]–[9] do not tackle the uncertainties that may arise in the future demands. In return, some studies consider this matter in different forms as follows. In [10], a two-stage approximate dynamic programming is proposed to determine the optimal charging strategy based on seamless short-term prediction and long-term estimation from historical data. Nevertheless, there is no guarantee that the demands will be met on departure time. Akhavan-Rezai *et al.* [11] predict near-future arrivals and their demands based on an artificial neural network and Markov Chain. Next, this prediction is fed to the optimization module to schedule the EVs request. Note that this prediction may not be accurate, and multiple sources of uncertainties may lead to many different scenarios.

Therefore, several studies model the future demands in the form of scenarios. Zhang *et al.* [12] design a novel type of charging station which allows multiple EVs to be connected to the same charger, but only one can charge at a time. Next, a two-stage stochastic optimization is developed to minimize the expected annual costs for providing charging services in different scenarios. Similarly, a recent study [13] extends the previous work [12] in terms of charging station design, i.e., multiple chargers can connect to multiple ports. Moreover, the studies [14]–[17] schedule the arriving EVs to parking-lot considering a small number (less than 1000) of scenarios as the future demands. In fact, the previous research [12]–[17] propose a two-stage stochastic model and limit the number of scenarios for future demands uncertainty to keep the problem computationally tractable.

In contrast to the two-stage stochastic model [12]–[17], our proposed multi-stage model is more consistent with the real situation of a parking-lot that the requests are realized at different times. In the finite time horizon, we can divide time into appropriate equal-length time-slots (or stages) that allow for recourse decisions at multiple stages of the charging schedule. A key feature of the multi-stage stochastic model is making a *non-anticipative* solution, i.e., the system makes decisions in each stage only regards to the realized information up to that stage. Moreover, this model is significantly harder to solve for a large scenario tree, corresponding to the exponential order of scenarios as the future demands.

Besides, the multi-stage stochastic optimization in the area of energy management is already addressed but limited to some topics. For example, hydro valleys management [18], hydropower scheduling [19], managing energy storage in micro-grids [20], and the commitment schedule of generation units [21] are addressed in this context. However, the problem model and time-independent of the random data in [18]–[21] make these solutions impractical for EVs time-dependent charging. For better comparison, let us consider a multi-stage model [20] in a micro-grid, solved by SDDP. This model determines electricity procurement and storage decision in response to the uncertainty of demand, renewable supply, and pricing information. Constant and already known numbers of buses are scheduled to satisfy independent demands in each stage, while here, inconstant and unknown numbers of EVs arrival in each stage should be scheduled in which demands may satisfy in multiple stages (i.e., time-dependency of each demand). Hence, to the best of our knowledge, the presented research is the first attempt towards extending this area to tackle EVs' time-dependent charging schedule by a multi-stage stochastic model.

Here, we focus on a public parking-lot that charges its visitors centrally. Each arriving user plugs the EV to the charging station and enters the departure time and energy demand in a smart-board. The Parking-lot Energy Management System (PLEMS) solves the AC problem quickly to admit the possible request; otherwise, suggests the maximum amount of energy. Moreover, the PLEMS solves the CS problem to take the admitted users into account periodically. To summarize, the key contributions of this study are as follows:

- We formulate a multi-stage linear stochastic programming to minimize the expected cost considering future demand uncertainty over the finite time horizon. The random data process for this problem contains the number of arrival users, their departing time and energy demand for each stage (or time slot). Here, our focus is on the

future demand uncertainty, but a prediction of Real-Time Pricing (RTP) based on the method [22] is employed to prevent the data process enlargement.

- To approximate the optimal solution by the so-called Sample Average Approximation (SAA) [23] problem, we discretize the random data process, corresponding to a finite scenario tree. Next, a tractable variant of well-known L-shaped [24], [25] decomposition for a large number of stages is employed, called SDDP [26], [27]. However, the SDDP procedure is not applicable due to time-dependent charging of EVs. To overcome this difficulty, we change and reformulate the model to enhance the SDDP procedure, named Time-dependent Stochastic Decomposition (TSD). It is noteworthy to mention that this multi-stage stochastic decomposition procedure is basically different from deterministic Dantzig-Wolfe decomposition applied to charge EVs in [28], [29].
- The PLEMS has multiple recourse opportunities to improve the solution as the information revealed gradually. The TSD procedure runs iteratively and generates the piece-wise linear outer approximation for the recourse function of each stage via the Bender's cuts. This cycle improves progressively to obtain a high-quality solution taking several hours that appears to be unsuitable for online solving. Consequently, the TSD procedure executes only once in the offline mode and collect the generated cuts to be used in the online mode. Hence, a linear programming problem is solved for the online mode to make it fast responsive, whether in the AC or the CS.
- In addition to the CS mechanism, an AC mechanism is proposed to guarantee the admitted users fulfilling the demands. Moreover, similar to the CS, the AC model considers the current and the future demands that leads to adjusting the unacceptable requests. That is, the future demands are modeled in the AC mechanism to prevent the earlier users do not capture all resources selfishly. On the other hand, considering the future demand in the CS mechanism results in saving the total cost as well as enough resources for the upcoming users.

The remainder of this paper is organized as follows. Section II presents the system model and describes a multistage linear stochastic problem. An iterative decomposition procedure is described in Section III for the offline and the online modes considering both the AC and the CS mechanisms. In Section IV, the simulation results are presented and compared with two approaches in different test cases. Section V concludes the paper.

II. Model Description

It is assumed a finite time horizon that is divided into equal-length time slots $\mathcal{T} = \{1, \ldots, T\}$. For notational convenience, we also define $\mathcal{T}' \equiv \mathcal{T} \backslash \{1\}$ to represent the time slots in which a recourse decision is made. The user $u \in U$ arrives in the time interval $[t-1, t)$, i.e., arrival time $a_u = t \in \mathcal{T}$, plugs the EV to the charging station and enters the status information, containing departure time (d_u) and energy demand (e_u), in a smart-board. Next, the PLEMS solves the AC problem, with regards to the current and the future demands, in order to admit the request that can fully supply. Otherwise, it offers the maximum amount of possible energy. At the end of the current time slot, the CS problem is solved again to schedule the admitted users for the next time slot.

Generally, the CS mechanism is designed to be solved in T different stages, each one corresponding to a time slot. The AC mechanism is also in a similar form to the CS except to be solved for each arriving EVs. In stage $t \in \mathcal{T}$, only the current users should be considered due to non-anticipative decision-making, while the future demands are also considered in the next stages $(t+1, \ldots, T)$. Thus, the problem aims at minimizing the expected cost of the current users, as well as uncertain future demands, subject to some operational limits. Therefore, the PLEMS deals with a multi-stage stochastic optimization as described in the following. Note that, we assume here the AC mechanism is not executed, i.e., there is no guarantee that the admitted users obtain entire demands in their departing time. However, this assumption in the final solution will be relaxed in the next section.

The random data process $\xi_t = (|U_t|, d_u, e_u : u \in U) \in \Xi_t$ denotes the number of arriving users, their departure time, and energy demands in stage $t \in \mathcal{T}'$, while the first stage is deterministic. In this definition, Ξ_t refers to the entire state space of the random data in the tth stage. The random data is realized before starting the tth stage, but for notational convenience, the same notation is applied; which one of them will be clear from the context.

In the first stage, a deterministic decision is made, and with the start of the second stage, a recourse one is fired and continued to the end of the time horizon. The recourse decision in stage $t \in \mathcal{T}'$ when ξ_t is realized, is denoted by $x_{u,t}(\xi_{[t]})$, where $\xi_{[t]}$ refers to the history of the random data realizations up to stage t. For notation simplicity and the fact that the charging power $x_{u,t}$ always depends on $\xi_{[t]}$, hereafter, we use the simple notation $x_{u,t}$.

Now we describe the operational limits in stage $t \in \mathcal{T}$. First, due to the physical limits of the local transformer of parking, the maximum total charging power is restricted to E^{max} in any time slot via

$$\sum_{u \in U_{[t]}} x_{u,t} \leq E^{max}, \quad t \in \mathcal{T}, \tag{1}$$

where the set $U_{[t]} = \{u \in U : t \in \mathcal{T}_u\}$, denotes all the existing users in the system up to stage t. In this regard, the set $\mathcal{T}_u = \{t \in \mathcal{T} : a_u \leq t \leq d_u\}$, shows the time horizon of the user u. Let the maximum charging rate per time slot depending on the EV model of user u be x_u^{max}, so the second constraint is

$$0 \leq x_{u,t} \leq x_u^{max}, \quad u \in U_{[t]}, t \in \mathcal{T}. \tag{2}$$

The last constraint should satisfy the admitted energy in the time horizon of each user. Given that the decision is made in different stages, we have

$$x_{u,t} \leq e_u - \bar{X}_{u,t-1}, \quad u \in U_{[t]}, t \in \mathcal{T}, \tag{3}$$

where $\bar{X}_{u,t-1}$ is the total allocated energy in the previous stages, which can be defined in the recursive form

$$X_{u,t} = x_{u,t} + \bar{X}_{u,t-1}, \quad u \in U_{[t]}, t \in \mathcal{T}.$$

Note that $X_{u,t}$ is initiated with $X_{u,0} = 0$ and $X_{u,\tau} = 0$ for $\tau \notin \mathcal{T}_u$. Moreover, the definition $X_t = (X_{u,t} : u \in U_{[t]})$ is used in the following. Since the constraint (3) is less than or equal, we penalize the uncharged amount of energies of each user at the departure time in the objective function later. Thereby, the set of feasible decisions $x_t = (x_{u,t} : u \in U_{[t]})$ in each stage $t \in \mathcal{T}$ is denoted by $\mathcal{X}_t = (\bar{X}_{t-1}, \xi_{[t]})$, and this set is defined by the constraints (1)-(3) for each $(\xi, t) \in \Xi \times \mathcal{T}$.

Let c_t and c^p denote per unit predicted price of electricity procured from the grid in time slot t and the penalty rate for the uncharged amount of energies, respectively. From the parking owner's point of view, the energy procurement cost and penalty cost should be minimized. Then, the objective function for the tth stage is reflected in

$$\mathfrak{c}_t x_t = \sum_{u \in U_{[t]}} c_t x_{u,t} + \sum_{\substack{u \in U_{[t]}, \\ d_u = t}} c^p \big(e_u - \bar{X}_{u,t-1} - x_{u,t}\big). \tag{4}$$

It is noteworthy to mention that the parking owner can make a particular profit by a mutual agreement with users. For example, the PLEMS gives users a bill at their departure time based on the actual charging cost plus a certain share as a profit. However, it is challenging to determine a fair price mechanism here, so the seamless integration of the pricing and charging mechanisms remains open for the future direction. Therefore, the multistage linear stochastic optimization can be represented in the nested form

$$\min_{x_1} \ \mathfrak{c}_1 x_1 + \mathbb{E}_{\xi_2}\Bigg[\min_{x_2} \mathfrak{c}_2 x_2 + \mathbb{E}_{\xi_3|\xi_{[2]}}\Bigg[\min_{x_3} \mathfrak{c}_3 x_3 + \cdots + \mathbb{E}_{\xi_T|\xi_{[T-1]}} \times \Bigg[\min_{x_T} \mathfrak{c}_T x_T\Bigg] \ldots\Bigg]\Bigg] \tag{5a}$$

$$\text{s.t.} \ \ x_t \in \mathcal{X}_t, \forall (\xi, t) \in \Xi \times \mathcal{T}, \tag{5b}$$

where $\mathbb{E}_{\xi_t|\xi_{[t-1]}}$ denotes the conditional expectation taken with regards to the conditional probability measure $\mathbb{P}_{\xi_t|\xi_{[t-1]}}$ in stage t. This nested structure indicates that multiple recourse opportunity is available to the PLEMS as the information revealed gradually over the planning horizon, consistent with the non-anticipative feature. Unfortunately, the problem (5) is computationally intractable, even for a moderate number of stages [27]. However, in the next section, the structure is amended and reformulated to a nested decomposition procedure to obtain high quality, approximate solutions.

III. The Decomposition Procedure

To start with, we replace the structure of the problem (5) by T stage dynamic programming in which the problem in stage $t \in \mathcal{T}$ when $\xi_{[t]}$ is realized, defined as

$$\mathcal{Q}_t\big(\bar{X}_{t-1}, \xi_{[t]}\big) = \min_{x_t \in \mathcal{X}_t} \mathfrak{c}_t x_t + \mathcal{Q}_{t+1}\big(X_t, \xi_{[t]}\big), \tag{6}$$

where

$$\mathcal{Q}_{t+1}\big(X_t, \xi_{[t]}\big) = \mathbb{E}_{\xi_{t+1}|\xi_{[t]}}\big[\mathcal{Q}_{t+1}\big(X_t, \xi_{[t+1]}\big)\big],$$

is the total expected future cost when the tth stage make a decision on X_t under realization $\xi_{[t]}$, also called the recourse function. Without loss of generality, we assume $\mathcal{Q}_{T+1}(\cdot) = 0$; however, any continuous and convex function can be applied.

Since the random data process ξ_t, $t \in \mathcal{T}'$, having continuous distributions, the problem cannot be computed in a closed-form solution [23], so needs to discretized the values. Therefore, a sample $\tilde{\xi}_t = (|\tilde{U}_t|, \tilde{d}_u, \tilde{e}_u : u \in U) \in \tilde{\Xi}_t$ is generated by using the well-known Monte-Carlo methods [30] to replace with the original or true distributions. These samples take a finite scenario tree into account, in which a node in stage $t = 1, \ldots, T-1$ has $j = 1, \ldots, N_{t+1}$ children,[1] touches each one with equal probability $\frac{1}{N_{t+1}}$. So the total number of scenarios, $N = \prod_{t=1}^{T} N_t$ ($N_1 = 1$), grows exponentially by increasing the number of stages.

Consequently, the true problem (6) is approximated by the so-called SAA [23] problem corresponding to a scenario tree. This problem in stage $t \in \mathcal{T}$, when $\tilde{\xi}_t^j$ is realized for $j = 1, \ldots, N_t$, is defined as

$$\tilde{\mathcal{Q}}_t^j\Big(\bar{X}_{t-1}, \tilde{\xi}_{[t]}^j\Big) = \min_{x_t \in \tilde{\mathcal{X}}_t^j} \tilde{\mathfrak{c}}_t x_t + \tilde{\mathcal{Q}}_{t+1}\Big(X_t, \tilde{\xi}_{[t]}^j\Big), \tag{7}$$

where the recourse function

$$\tilde{\mathcal{Q}}_{t+1}\Big(X_t, \tilde{\xi}_{[t]}^j\Big) = \frac{1}{N_{t+1}} \sum_{j'=1}^{N_{t+1}} \tilde{\mathcal{Q}}_{t+1}^{j'}\Big(X_t, \tilde{\xi}_{[t+1]}^{j'}\Big),$$

can be calculated. Similarly, $\tilde{\mathcal{Q}}_{T+1}(\cdot) = 0$ is assumed.

L-shaped [24], [25] is a general and well-known nested decomposition that can be applied to solve the problem (7) via an iterative procedure. The procedure consists of two main steps, a forward pass, and a backward pass. The former originates at the tree root, solves the problem and saves the decisions to be used for the next stage. This step progressively solves all of the nodes in the order of stages, and at the end, a feasible solution obtains to calculate the upper bound ($\bar{z}$). In return, the backward pass proceeds from the last stage to the first stage to generate the piece-wise linear outer approximation for the recourse function via the Bender's cuts. Therefore, Solving the problem in the root yields the lower bound ($\underline{z}$). The procedure terminates whenever $\underline{z}$ sufficiently converges to $\bar{z}$.

As mentioned above, the L-shaped solves $N' = \sum_{\tau=1}^{T}(\prod_{t=1}^{\tau} N_t)$ problems, i.e., equal to the total number of tree nodes, in a forward or backward pass which grows exponentially by increasing the number of stages. Therefore, this procedure is computationally intractable, even for a moderate number of stages. If the random data process is *stage-wise independent*, i.e., the random vector $\tilde{\xi}_{t+1}$ is independent of $\tilde{\xi}_{[t]}$, a tractable variant of this procedure can be applied, called SDDP [26], [27]. In a public parking lot, the arriving users in a stage usually have the requests which are independent of the others in the upcoming stages; hence, we take the stage-wise independent assumption hereafter.

The SDDP procedure is similar to the L-shaped with some changes as follows. In the forward step, $M \ll N$ scenarios

[1]For simplicity, the number of children of all nodes in the same level assumes equal, but this assumption will be realized in the following.

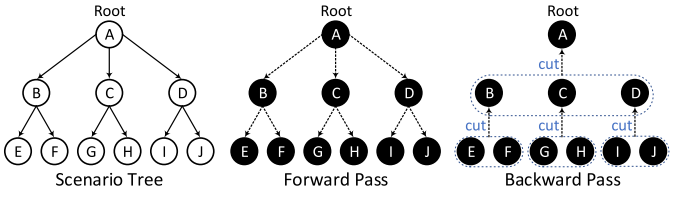

(a) L-shaped procedure.

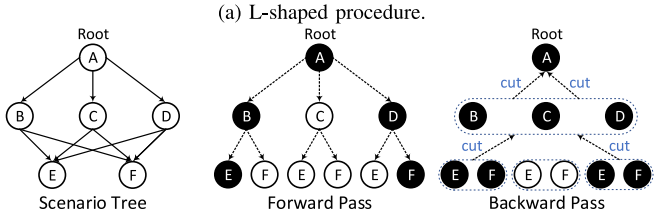

(b) SDDP procedure when $M = 2$.

Fig. 1. Illustration of two scenario trees with three stages and six scenarios.

are randomly selected to solve MT problems in total. Note that each node j in stage $t \in \mathcal{T}'$, has the same children in stage $t+1$,[2] thanks to the stage-wise independent assumption, so the same recourse function. Therefore, for a scenario in stage $t = T, \ldots, 2$, in the backward pass, all nodes in t, N_t problems, are solved to generate a cut for the recourse function of the stage $t-1$ ($\tilde{\mathcal{Q}}_t(\cdot)$). This cut is valid for all nodes in stage $t-1$. Consequently, $M(\sum_{t=2}^{T} N_t) + 1$ problems solve in the backward pass, having a linear relationship with the number of stages. It is noteworthy to mention that the SDDP procedure yields a statistical upper bound and a deterministic lower bound in the forward and the backward step, respectively (more details in [27]). Fig 1 illustrates the L-shaped and the SDDP procedures in similar scenario trees with three stages and six scenarios.

To apply the SDDP procedure to the problem (7) in stage $t \in \mathcal{T}'$ and node $j = 1, \ldots, N_t$, we first take the stage-wise independent assumption into account. It leads to some changes in the problem formulation to work the above procedure correctly. Due to $\mathbb{P}_{\xi_t|\xi_{[t-1]}} = \mathbb{P}_{\xi_t}$ and $\mathbb{E}_{\xi_{t+1}|\xi_{[t]}} = \mathbb{E}_{\xi_{t+1}}$ in the SDDP-type problems, the objective function $\tilde{\mathcal{Q}}_t^j(\cdot)$ depends on the realization $\tilde{\xi}_t^j$, not the history, while the recourse function $\tilde{\mathcal{Q}}_{t+1}(\cdot)$ is independent of $\tilde{\xi}_t^j$. However, these changes are not applicable here, because the current users in the stage t may have arrived in the previous stages. Consequently, the random data process depends on the history (according to (1)-(4), $u \in U_{[t]}$) and does not meet the SDDP requirements.

In other words, these coupling of multiple stages has difficulty in the backward pass of the SDDP. Suppose the node $j' = 1, \ldots, N_t$, in the backward pass that does not touch in the forward, as a result, a set of new users should be considered that they depend on the future stages. These dependencies can be extended to the end of the time horizon. For better illustration, assume a scenario A-B-E is selected in the forward pass of the SDDP procedure, as shown in Fig 1(b). Next, in the second stage of the backward pass, the users of node C and D are also taken into account that they have different numbers and requests compared to the users of node B. However, the users of node B is also considered in the third stage, but the users of node C or D only in the second stage. In this case, we need to set $M = N$ that converts the problem to the intractable L-shaped procedure.

However, we can remove the dependency of the random data process to the history by changing the problem and reformulation. The main idea is that the arriving users in each stage, schedule over the entire time slots, all at once. As a result, the users of one stage will no longer be in the next stages to keep the stage-wise independent assumption as well as non-anticipative feature. Henceforth, we define new symbol $\mathcal{S} = \{1, \ldots, S\}$ denotes the stages, each one corresponding to a time slot ($T = S$), also keep the symbol t for time slots. Note that, all sets, parameters, and variables were dependent on stages till now, that do not redefine here. Now, we have to amend the constraints (1)-(4) and reformulate the problem (7) to construct a time-dependent SDDP procedure, named TSD.

To do so, for stage $s \in \mathcal{S}$ and node $j = 1, \ldots, N^s$, when $\tilde{\xi}^{s,j}$ is realized, the following constraints and the objective function are superseded with their counterparts. First, the inequality (1) for the physical limits of the local transformer for each time slot is rewritten to

$$\sum_{\substack{u \in \tilde{U}^{s,j}, \\ t \in \tilde{\mathcal{T}}_u}} x_{u,t} \le E^{max} - \bar{X}_t^{s-1} : (\pi_t), \quad t \in \mathcal{T}^s, \tag{8}$$

where $\bar{X}_t^{s-1}$ denotes the total amount of assigned energy before the current stage s for each time slot $t \in \mathcal{T}^s$. Generally, X_t^s defines in the recursive form

$$X_t^s = \sum_{\substack{u \in \tilde{U}^{s,j}, \\ t \in \tilde{\mathcal{T}}_u}} x_{u,t} + \bar{X}_t^{s-1}, \quad s \in \mathcal{S}, t \in \mathcal{T}^s,$$

with the initial value $\bar{X}_t^0 = 0$. In this definition, the set $\mathcal{T}^s = \{t \in \mathcal{T} : t \ge s\}$ represents the time slots after the stage s, and set $\tilde{U}^{s,j}$ denotes the realized users in stage s and node $j = 1, \ldots, N^s$. In general, the variable defines after the colon refers to the dual variable corresponding to that constraint. Furthermore, the maximum charging rate of the EV's battery u per time slot (2), the user demand in the time horizon (3) and the objective function along with the penalty term (4), are reflected in order in

$$0 \le x_{u,t} \le x_u^{max}, \quad u \in \tilde{U}^{s,j}, t \in \tilde{\mathcal{T}}_u, \tag{9}$$

$$\sum_{t \in \tilde{\mathcal{T}}_u} x_{u,t} \le \tilde{e}_u, \quad u \in \tilde{U}^{s,j}, \tag{10}$$

$$\tilde{\mathfrak{c}}^s x^s = \sum_{u \in \tilde{U}^{s,j}} \sum_{t \in \tilde{\mathcal{T}}_u} \big(c_t x_{u,t} + c^p \big(\tilde{e}_u - x_{u,t} \big) \big). \tag{11}$$

Note that, receiving requests in the AC mechanism, have to be checked for admission, follow the described model. However, for each admitted user in the AC or the CS mechanism, we convert the inequality (10) to equality in order to satisfy the user demand, and drop the penalty term from the objective function (11) as well. Therefore, the AC and the CS mechanisms are both applicable here with the difference mentioned in the constraint (10) and the objective (11).

[2]Now, the previous assumption about the same number of children is realized.

Now, we define the set of feasible decisions $x^s = (x_{u,t} : u \in \tilde{U}^{s,j}, t \in \mathcal{T}^s)$ in each stage $s \in \mathcal{S}$ with the symbol $\tilde{\mathcal{X}}^{s,j} = (\bar{X}_t^{s-1}, \tilde{\xi}^{s,j} : t \in \mathcal{T}^s)$. This set consists of the constraints (8)-(10) for each $(\tilde{\xi}, s) \in \tilde{\Xi} \times \mathcal{S}$. Consequently, the problem (7) can be reformulated as

$$\tilde{Q}^{s,j}\left(\bar{X}_t^{s-1}, \tilde{\xi}^{s,j}\right) = \min_{x^s \in \tilde{\mathcal{X}}^{s,j}} \tilde{\mathfrak{c}}^s x^s + \tilde{\mathcal{Q}}^{s+1}(X_t^s), \tag{12}$$

where the recourse function is

$$\tilde{\mathcal{Q}}^{s+1}(X_t^s) = \frac{1}{N^{s+1}} \sum_{j'=1}^{N^{s+1}} \tilde{Q}^{s+1,j'}\left(X_t^s, \tilde{\xi}^{s+1,j'}\right).$$

Our objective is to solve the problem (12) by approximating the recourse function by the Benders' cuts. Suppose the procedure in ith iteration and in stage $s \in \mathcal{S}$ of the backward pass; then we replace the current cuts $\mathfrak{Q}_i^{s+1}(\cdot)$ with $\tilde{\mathcal{Q}}^{s+1}(\cdot)$ in this problem. Now, we can solve the problems $\tilde{Q}^{s+1,j}(\cdot)$ for all $j = 1, \ldots, N^{s+1}$, in the stage $s+1$ of the backward pass to create a new cut $l^{s+1}(X_t^s)$ for the previous stage s. Next, the current cuts are updated based on $\mathfrak{Q}_{i+1}^{s+1}(X_t^s) = \max(\mathfrak{Q}_i^{s+1}(X_t^s), l^{s+1}(X_t^s))$. Finally, the general structure of the cuts that are developed by the Bender's cut (the subgradient inequality) is

$$\begin{aligned} l^{s+1}(X_t^s) &= \alpha^{s+1} + \sum_{t \in \tilde{\mathcal{T}}^s} \beta_t^{s+1} X_t^s \\ &= \alpha^{s+1} + \sum_{t \in \tilde{\mathcal{T}}^s} \sum_{\substack{u \in \tilde{U}^{s,j}, \\ t \in \tilde{\mathcal{T}}_u}} \beta_t^{s+1} x_{u,t} + \sum_{t \in \tilde{\mathcal{T}}^s} \beta_t^{s+1} \bar{X}_t^{s-1}, \end{aligned} \tag{13}$$

where we will express how to calculate the constant coefficient, α^{s+1}, and the variable coefficients, β_t^{s+1}, later. In this equation, the last equality is obtained from the replacement of X_t^s in the middle equality. Finally, the problem (12) in stage $s \in \mathcal{S}$ and the node $j = 1, \ldots, N^s$, considering the generated cuts in the form of (13), can be converted to

$$\tilde{Q}^{s,j}\left(\bar{X}_t^{s-1}, \tilde{\xi}^{s,j}\right) = \min \tilde{\mathfrak{c}}^s x^s + \theta^{s+1} \tag{14a}$$

$$\text{s.t.} \quad \theta^{s+1} \geq \alpha_k^{s+1} + \sum_{t \in \tilde{\mathcal{T}}^s} \sum_{\substack{u \in \tilde{U}^{s,j}, \\ t \in \tilde{\mathcal{T}}_u}} \beta_{t,k}^{s+1} x_{u,t} + \sum_{t \in \tilde{\mathcal{T}}^s} \beta_{t,k}^{s+1} \bar{X}_t^{s-1} : \tag{14b}$$

$$(\rho_k), k \in \mathcal{K}^{s+1}, \tag{14b}$$

$$(8), (9), (10), \tag{14c}$$

where $\mathcal{K}^{s+1}$ represents all the cuts have been added to stage $s+1$ up to the current iteration.

Let the optimal value of the objective function of the problem (14) in $(s+1)$th stage and node $j = 1, \ldots, N^{s+1}$, are denoted by $\underline{\tilde{Q}}^{s+1,j}(\cdot)$. Furthermore, the optimal values for the dual variables are denoted by the symbols $\underline{\rho}_k^{s+2,j}$, for $k \in \mathcal{K}^{s+2}$ and $\underline{\pi}_t^{s+1,j}$, for $t \in \tilde{\mathcal{T}}^{s+1}$, respectively. Accordingly, the coefficients of the equality (13) can be obtained by

$$\alpha^{s+1} = \frac{1}{N^{s+1}} \sum_{j=1}^{N^{s+1}} \underline{\tilde{Q}}^{s+1,j}(\cdot) - \sum_{t \in \tilde{\mathcal{T}}^{s+1}} \beta_t^{s+1} \bar{X}_t^s, \tag{15}$$

Algorithm 1: The TSD Procedure

Initialize: $i \leftarrow 1, \underline{z} \leftarrow -\infty$, $\{\bar{z}_{avg}, \bar{z}_h\} \leftarrow +\infty$
1 **while** *some stopping criterion is not satisfied* **do**
2 Sample M scenarios $\tilde{\Xi}_i = \left\{\tilde{\xi}_m^1, \ldots, \tilde{\xi}_m^S\right\}_{m=1,\ldots,M}$
3 (Forward step)
4 **for** $m = 1, \ldots, M$ **do**
5 **for** $s = 1, \ldots, S$ **do**
6 solve (14): save $\bar{x}_m^s$, $\bar{X}_{t,m}^s$
7 $\bar{z}_m \leftarrow \sum_{s \in \mathcal{S}} \tilde{\mathfrak{c}}^s \bar{x}_m^s$
8 (Upper bound update)
9 $\bar{z}_{avg} \leftarrow \frac{1}{M} \sum_{m=1}^{M} \bar{z}_m$
10 $\sigma^2 \leftarrow \frac{1}{M-1} \sum_{m=1}^{M} \left(\bar{z}_m - \bar{z}_{avg}\right)^2$
11 $\bar{z}_h \leftarrow \bar{z}_{avg} + 1.96 \frac{\sigma}{\sqrt{M}}$
12 (Backward step)
13 **for** $m = 1, \ldots, M$ **do**
14 **for** $s = S, \ldots, 2$ **do**
15 **for** $j = 1, \ldots, N^s$ **do**
16 solve (14) using $\bar{X}_{t,m}^{s-1}$: save $\underline{Q}_m^{s,j}(\cdot)$, and $(\underline{\rho}_{k,m}^{s,j}, \underline{\pi}_{t,m}^{s,j})$
17 update $\mathcal{K}^s$ with coefficients $(\alpha_m^s, \beta_{t,m}^s)$
18 (Lower bound update)
19 $\underline{z} \leftarrow \underline{Q}^1(\cdot)$ // solve (14) in stage 1
20 $i \leftarrow i + 1$

$$\beta_t^{s+1} = \frac{1}{N^{s+1}} \sum_{j=1}^{N^{s+1}} \left(\sum_{k \in \mathcal{K}^{s+2}} \underline{\rho}_k^{s+2,j} \beta_{t,k}^{s+2} - \underline{\pi}_t^{s+1,j} \right). \tag{16}$$

It is noteworthy to mention that the coefficients β_t^{s+1} are the gradient of $\tilde{Q}^{s+1,j}(\cdot)$ at $\bar{X}_t^s$ that can be calculated by the corresponding dual problem. Thus, the steps of the TSD procedure are summarized in the algorithm (1).

A common stopping criterion of such Benders' decompositions (or SDDP-type algorithms) is the lower bound sufficiently converges to the upper bound. For example, the Lines 9 to 11 of the algorithm (1) state that the actual upper bound is lower than $\bar{z}_h$ with the confidence of about 95% (more details in [23]). However, further precautions need to be considered for the *statistical* upper bound. As another criterion, the lower bound starts to be stabilized, and $\bar{z}_h$ sufficiently converges to that. The minimum number of iterations is also considered [27], [31].

Many heuristics in the literature are proposed to improve the performance of such SDDP-type decomposition (see [32]), and here we select one. As the TSD iterations proceed, many cuts are generated, but all of which are not active at each stage. To speed up the problem solving, we add the cuts iteratively as needed instead of keeping all together. This cutting selection heuristic, called Dynamic Cut Selection (DCS), is employed here and can be integrated into the TSD procedure (see the implementation details about the DCS in [32]).

The last obstacle to be removed is how to run the TSD procedure, i.e., the algorithm (1), as the AC and the CS

TABLE I
ELECTRIC CHARACTERISTICS OF POPULAR EV MODELS [33], [34]

Model	Battery Capac. [kWh]	L2C / DCFC rate [kW]	Avg Energy Cons. per 100 mi [kWh]
Tesla Model 3	55	11 — 100	23.8
Nissan Leaf	40	6.6 — 50	26.4
Volkswagen e-Golf	36	7.2 — 40	27.0
BMW i3	33	7.7 — 50	25.7
Hyundai Ioniq Elec.	28	7.0 — 100	23.3
Honda Clarity Elec.	25	6.6 — 40	28.0
Ford Focus Elec.	23	6.6 — 50	27.8
Mitsubishi i-MiEV	16	3.7 — 40	25.9

mechanisms work correctly. An approach for stage $s \in \mathcal{S}$ is suggested so that we have a tree with $S - s$ stages in which all of the current users up to stage s are considered in the root. Therefore, the TSD procedure is required to be executed for each run of both mechanisms. Although this approach can obtain a better solution compared to the upcoming approach, each run of the TSD takes several hours to reach a high-quality solution. Consequently, this approach is not applicable in this manner.

Here, we apply the alternative approach has been used in the SDDP-type algorithms [20], which solves the TSD procedure only once in the *offline* mode, and collects the generated cuts to be used in the *online* mode. For arriving users in the sth stage in the online mode, if their requests are perfectly matched a node $j = 1, \ldots, N^s$, then it is adequate to solve the problem (14) along with obtained cuts in the offline mode, whether in the AC or the CS. Note that, the higher the node numbers, the more likely this assumption occurs. Otherwise, we can still solve the problem (14) with the offline cuts, because the general structure of the cuts, defined in (14b), only depends on $\bar{X}_t^{s-1}$ that is available in stage s. Furthermore, there is no difference that we are in the forward pass of the offline mode or the online mode because we make a decision based on the current realized random data (non-anticipative feature), so the generated cuts are valid. Consequently, each run of the AC or the CS in the online mode is equivalent to the problem (14) solved once, that is fast responsive.

IV. SIMULATION RESULTS

Here, parking near commercial places is assumed to serve EVs charging between 8 a.m. and 11 p.m., including 60 time-slots of 15 minutes for the online mode. On the contrary for the offline mode, a time slot is added before the time horizon started, i.e., 61 time-slots or stages, as the root of the scenario tree, without any EV's arrival. In Table I, we consider multiple popular EV models randomly arrived at parking with different electric characteristics, containing battery capacity, charging rate of Level 2 charger (L2C) or DC fast charger (DCFC), and average energy consumption per 100 miles.

Due to the lack of information on real-world users' behavior in parking with EV's charging stations, we use a publicly available parking dataset from the Melbourne Data Platform [35], as well as the NHTS survey 2017 of travel behavior [36] to create simulations that are closer to reality. Therefore, the data of arrivals and departures are collected from the West Melbourne area by in-ground parking-lot sensors with a capacity of 62 cars. The invalid and small parking duration is also omitted from the dataset. We assume the state of charge (SoC) of each EV at the start of a day lies in the range of 50% to 100%, and users make some trips before arriving at parking. According to NHTS 2017 [36], on average, each car makes 2.7 trips daily, each one 9.55 miles length. Moreover, the hourly distribution of trips by the time of day allows the entire trips' length of each EV can be calculated, so the total energy consumption. Consequently, the user demand is set to the empty amount of battery capacity unless the user's presence time in parking limits that.

According to the above procedure, we create three different scenario trees for the offline mode so that the tree node numbers, N^s, hold constant for all $s = 2, \ldots, S$, and is selected to be 5, 10, or 15. Moreover, 200 different online samples are generated that are considered the same for different settings. We also consider the parking data on Fridays, Aug 2016, for the scenario trees, while the online samples are generated based on Fridays, Sep 2016. For better illustration of the users' behavior trend, the arrival rate and the average waiting time on Friday 9$^{\text{th}}$ Sep 2016 are shown in Fig. 2(a). Note that the waiting time reflects how many time slots that the EVs stay in the system. Finally, the last setting is pricing and its prediction. The real-time pricing was obtained from PJM Interconnection [37], and it is predicted according to the method [22], as shown in Fig. 2(b) on Friday 9$^{\text{th}}$ Sep 2016. The penalty rate is also set to \$100/MWh for rejected demands.

All results are obtained from a 14 core processor Intel Xeon E5-2695, with a 64 GB RAM Windows machine. Moreover, the problems execute in parallel on the *ParFor* loop of the MATLAB 2018a software and solved by Gurobi 8.1 solver. For Algorithm (1), 13 parallel programs with four samples are dedicated to the forward and the backward passes, i.e., $M = 52$, and another one for aggregation of the non-duplicate cuts. The algorithm terminates if either the $\underline{z}$ stabilizes and sufficiently converges to $\bar{z}_h$ by a factor of 0.01, or 300 iterations complete, whichever occurs first (In Gurobi solver, we manually set the default gap to zero without manipulating the other default settings). Note that the execution time has a linear relationship with the number of CPU cores that all reported times here are valid for a 14-core processor computer.

In the following, we assess the impact of different parameters on the quality of solutions in L2C or DCFC categories. In each test case, the generated cuts in the offline mode are saved to employ for the online mode. For a complete evaluation, the online samples are compared with Perfect Foresight (PF) and myopic approaches. The PF approach is the theoretical optimal solution that knows all stochastic parameters *a priori*. In contrast, the myopic ignores future demands and reschedules based on the present requests in each stage. Note that the AC mechanism is also implemented in both. Furthermore, we compare these approaches in terms of total cost, including the energy cost plus penalty cost of rejected demands, and rejected demands in the following. In general, the fewer demands are rejected, the more satisfied users, which in turn has a significant impact on the profitability of the parking owner. Therefore, users' satisfaction is reflected in both total cost and rejected demand terms.

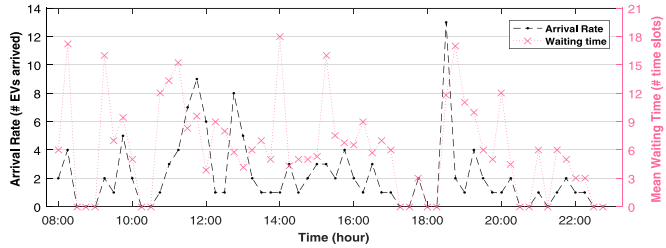

(a) Arrival rate and Waiting Time

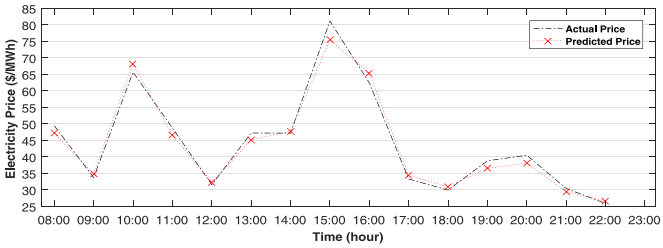

(b) RTP and its prediction

Fig. 2. Users' behavior and electricity price over the time horizon on Friday 9th Sep 2016.

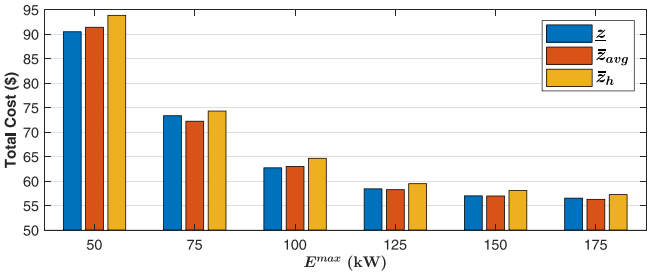

Fig. 3. The Cost of Offline Mode in Level 2 Charging Station when $N^s = 5$.

A. The Effect of E^{max} on Level 2 Charging Station

The local transformer capacity (E^{max}) have a significant impact on rejected demands and energy procurement cost. The higher the value, the better the solution quality, but it can increase the investment cost unreasonably and have a devastating effect on the grid's stability. Here, we take a wide range of E^{max} values varied from 50 kW (i.e., 12.5 kWh/15min) to 175 kW in increments of 25 kW, which is equivalent to a charge of about 7 to 26 Nissan Leaf in parallel at the maximum rate.

The total cost, in terms of the lower and the statistical upper bounds in dollars, is shown in Fig. 3 for the offline mode. To reduce the high variation of the statistical upper bound, we average the last 20 iterations and report in all test cases; however, the different samples can change the gap within two percent range. Since the PF solution is the theoretical optimal value, the gap between the other two approaches and the PF is reported in the online mode in all test cases. Therefore, the percentage of cost gap and the value of the rejected energy gap for the online samples are represented in Fig. 4(a) and Fig. 4(b), respectively. As seen in Fig. 4, box plots of the TSD are closer to the PF solution, as well as more stable compared to the myopic approach, especially in the mid-range of E^{max} values that makes the charging schedule more challenging.

B. The Effect of N^s on Level 2 Charging Station

In general, the higher the number of nodes in the scenario tree, the better the output if the samples are well extracted based on the Monte-Carlo. In this test case, we select the mid-range of E^{max} in the previous test case to evaluate the effect of N^s. Therefore, the offline results over the scenario trees are shown in Table II, in terms of the lower and the upper bounds in dollars, the approximate gap percentage between $\underline{z}$ and $\bar{z}_h$,

TABLE II
THE OFFLINE RESULTS IN LEVEL 2 CHARGING STATION

E^{max}	N^s	$\underline{z}$	$\bar{z}_{avg}$	$\bar{z}_h$	Gap %	# of Cuts	Time/iter
75	5	73.33	72.21	74.28	1.30	339040	4.32
	10	73.44	72.14	74.20	1.02	389540	9.06
	15	73.49	72.17	74.26	1.04	411389	12.98
100	5	62.69	62.97	64.64	3.11	365380	4.20
	10	62.80	62.70	63.91	1.76	382934	9.13
	15	62.88	62.67	63.84	1.51	412839	12.93
125	5	58.40	58.23	59.45	1.80	241144	3.66
	10	58.54	58.25	59.40	1.46	299600	6.45
	15	58.66	58.20	59.37	1.21	345261	10.24
150	5	56.97	56.94	58.06	1.91	144672	2.77
	10	57.36	57.15	58.30	1.63	202900	5.41
	15	57.45	57.02	58.26	1.40	204292	8.52

TABLE III
THE ONLINE RESULTS IN LEVEL 2 CHARGING STATION

E^{max}	N^s	Total Cost	Gap (mean|variance)%		Rejected Energy (kWh)		
		PF	Myopic	TSD	PF	Myopic	TSD
75	5	72.09	5.22|1.96	0.87|0.33	267.8	351.1	276
	10			0.74|0.30			274.7
	15			0.70|0.31			274.2
100	5	60.47	7.26|2.10	1.51|0.35	82.3	168.4	99
	10			1.36|0.27			97.8
	15			1.31|0.28			96.3
125	5	54.36	5.69|2.78	1.64|1.35	2.2	47.6	17.1
	10			1.67|1.31			19.1
	15			1.52|1.29			15.2
150	5	52.92	1.58|1.36	0.69|0.37	0.04	2.1	2.9
	10			0.69|0.36			2.7
	15			0.68|0.37			2.6

the number of non-duplicate cuts, and the average time per iteration in minutes. The table indicates that the number of further nodes results in the improvement of the lower bound and the gap percentage that lies in the appropriate range in all values. Moreover, a linear relationship between the time consumption and N^s can be found (as discussed in Section III) that the number of non-duplicate cuts somewhat affected. For example, $E^{max} = 75$ and 100 create more challenges compared to the other values, so generate more cuts and consume more time.

Furthermore, Table III reflects the online results in terms of total cost and rejected energy. Since the PF cost is the absolute minimum, the average value is reported directly in dollars, and the mean and the variance gap percentage between two other approaches and the PF is calculated. The table shows the superiority of the TSD over the myopic in terms of a mean

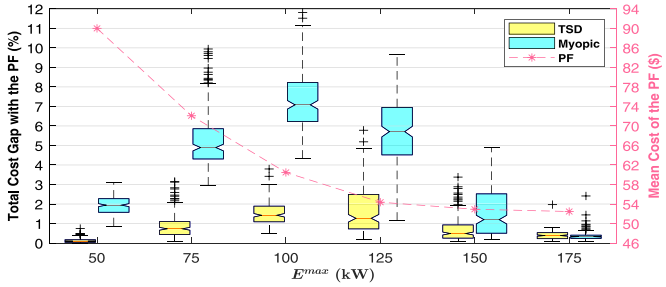

(a) Cost Gap with the PF approach

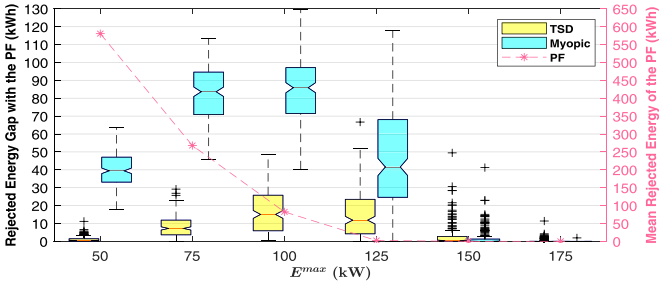

(b) Rejected Energy Gap with the PF approach

Fig. 4. Box Plots of the Online Mode in L2Cs when $N^s = 5$.

TABLE IV
THE OFFLINE RESULTS IN DC FAST-CHARGING STATION WHEN $N^s = 10$

E^{max}	$\underline{z}$	$\bar{z}_{avg}$	$\bar{z}_h$	Gap %	# of Cuts	Time/iter
75	68.67	67.59	69.75	1.56	265604	6.52
100	56.14	55.73	57.12	1.74	306898	7.01
125	50.60	49.79	51.02	0.84	288064	6.71
150	48.17	47.87	48.86	1.42	278582	6.68

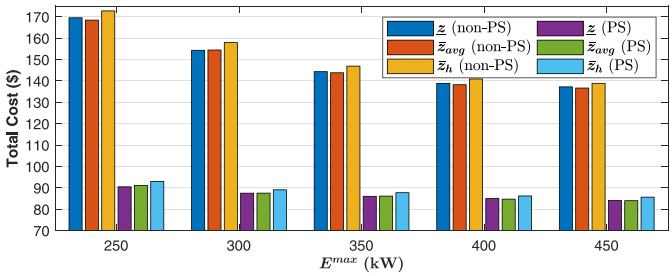

Fig. 5. The Cost of DCFC Offline Mode in PS and non-PS when $N^s = 10$.

gap, as well as low variance, which demonstrates the solution stability. Also, in most values, increasing N^s reduces the gap. On the other hand, since the PF may accept all requests, the mean and the variance gap percentage tends to infinity; hence, the mean rejected energies is only reported. These outputs confirm the previous achievement, too.

C. The Effect of Charging Station Upgrade to DCFC

Because DCFCs have a much higher charging rate than L2Cs, they can support more requests in the most cost-effective and less time-consuming way. It is a notably better option for parking that users have a shorter presence time than their charging time. However, this option can impose much more investment costs on the parking owner, which requires comprehensive cost-benefit analysis as discussed in the next subsection. Here, we run two different test cases with DCFCs. The first one shows the impact of the higher charging rate of this station compare to the previous test case, and the second one increases the demands and the local transformer capacity to achieve more realistic situations for two different cases; price sensitive (PS) and non-PS users. Note that we assume the maximum rate of DCFCs are limited to 50 kW to get better matches on most available chargers and EVs. Furthermore, we select $N^s = 10$ in the following test cases since it makes better solutions in a reasonable time, as seen from Section IV-B.

Now we take the first test case into account that has the same settings as the previous test case in Section IV-B to evaluate the effect of increasing the charging rate. Tables IV and V show the results of the offline and online modes, respectively. Comparison of results with Tables II and III indicate that the TSD outputs are significantly improved in all aspects, while the myopic is degraded. Due to the fact that the charging time is shorter than L2Cs and the myopic does not consider future demands, it waits more time to arrive at the less expensive electricity cost while having to reject more new demands. However, the TSD makes better use of low-cost charging time with regards to future demands.

In the second test case here, we increase the users' demand because it can be supported by DCFCs in a short time. Therefore, the SoC of each EV at the start of a day changes to the range of 10% to 50% without changing the other parameters. For better evaluation, we also take a new case into account that users are assumed to be price sensitive. However, due to limited available data of users' demand in a real parking, similar to references [15], [38], we assume that users' demand and RTP are related through a linear function. Therefore, user u requests at least 20% of the battery's empty capacity (e_u^{max}) which more than that, depends on the average RTP of the user presence time in parking (c_u^{avg}), as defined in

$$e_u^{\text{PS}} = \max\left(0.2, \frac{c^{max} - c_u^{avg}}{c^{max} - c^{min}}\right) \times e_u^{max}, \tag{17}$$

where c^{max} and c^{min} denote the maximum and minimum RTP, respectively. Note that, in another case that users who are not price sensitive, we set $e_u^{\text{non-PS}} = e_u^{max}$ for all users. Accordingly, we need to generate a new scenario tree for the offline mode and 200 new online samples following new demands based on the aforementioned equations. Next, we take a wide range of E^{max} values varied from 250 kW to 450 kW. Therefore, Fig. 5 shows the cost of offline results, and Fig. 6 illustrates the box plots of the online results gap between the other two approaches and the PF approach. These outputs indicate the narrow gap between the TSD and the PF approach; also stability compared to the myopic approach in both PS and non-PS cases. Comparing the results of the PS case with the non-PS case reveals that, on average, users' demand decreases by only 48% while the total cost improves by 74%, as well as reasonable decrease of the rejected demands.

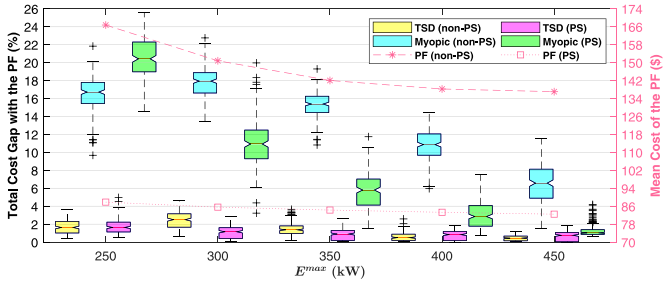

(a) Cost Gap with the PF approach

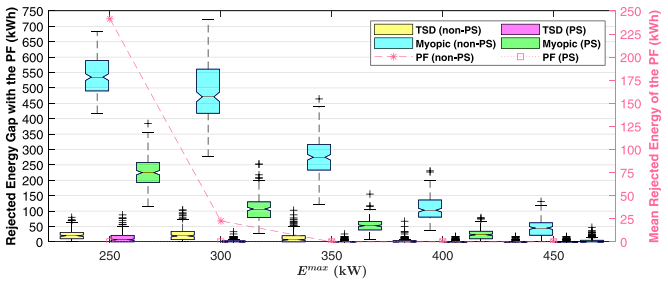

(b) Rejected Energy Gap with the PF approach

Fig. 6. Box Plots of the DCFC Online Mode in PS and non-PS cases when $N^s = 10$.

TABLE V
THE ONLINE RESULTS IN DC FAST-CHARGING STATION WHEN $N^s = 10$

E^{max}	Total Cost $	Gap (mean|variance)%		Rejected Energy (kWh)		
	PF	Myopic	TSD	PF	Myopic	TSD
75	69.95	9.17|4.57	0.30|0.04	230.3	369.6	230.8
100	55.99	17.29|6.15	2.18|0.79	17.24	199.27	30.17
125	50.53	16.24|2.80	1.45|0.35	0	91.44	6.07
150	48.59	10.87|6.24	0.34|0.13	0	36.97	1.27

D. Cost-Benefit Analysis

As discussed and demonstrated in the previous subsection, DCFCs can support more requests and significantly improve users' satisfaction compared to L2Cs. However, the cost-benefit analysis can provide a suitable benchmark for the parking owner to choose the best solution over an extended period. Here, without manipulating the other parameters, we set the EVs' SoC at the start of a day to the mid-range of 25% to 75%, and E^{max} values in range of 100 kW to 350 kW over 5-years online samples.

To calculate the profit of parking owner, we need to consider the investment cost (IC), energy procurement from the grid, i.e., energy cost (EC), and selling energy to users, i.e., energy income (EI). First, the IC includes L2C or DCFC unit costs, installation costs, maintenance, and networking costs. To reduce the IC due to the large number of charging stations, we assume that basic pedestal dual-port DCFC (and dual-port L2C) units with a hardware cost of 14000$ (3000$) and an installation cost of 9000$ (1500$) are mounted, each one requires 200$ (75$) per month networking and maintenance fee [39]. Second, the EC is calculated based on RTP. Third, among different business models for calculation of EI, we take the Tesla kWh pricing into account in the United States that users pay $0.28/kWh [40]. It is worth mentioning that in the following, we report the cost/income values separately so that the readers can replace each with their desired values.

Fig. 7 shows the cost-benefit analysis over a medium-term period (5-years) to compare the impact of L2Cs and DCFCs infrastructures among three different approaches for a wide range of transformer capacity. These outputs indicate that the IC accounts for a significant part of the costs, particularly in DCFCs, which would only be offset over a longer period of time. For example, with this level of infrastructure, the TSD would not yield positive profit until the second year of L2Cs operation, while this would occur after 4 years for DCFCs ($E^{max} \geq$ 200kW). However, in case of long-term operation (over 10 years), the parking owner not only would benefit more from DCFCs than L2Cs, but also satisfy more users' demand ($E^{max} \geq$ 200kW). Finally, the TSD would make more profit than the myopic approach, as well as the results close enough to the PF.

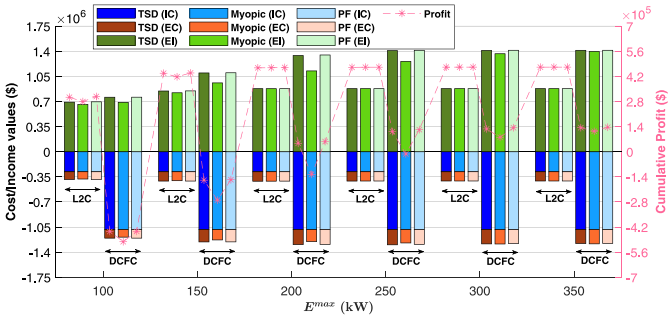

Fig. 7. Cost-benefit analysis over 5-years online samples.

V. CONCLUSION

In this research, we model a multi-stage stochastic linear programming to minimize the expected total energy costs over the finite time horizon. The model includes three sources of uncertainty related to future demands, subject to some operational limits, including the local transformer capacity limits, the maximum acceptance rate of the EV's battery, and user demands. Next, we approximate the model using the SAA problem, which is corresponding to a finite scenario tree. Since the SAA is computationally intractable, even for a moderate number of stages, we propose the TSD procedure to be consistent with time-dependent allocation; an amendment of well-known SDDP procedure. The TSD procedure takes several hours to obtain a high-quality solution; hence, we run it in the offline mode and collect the generated cuts to be used in the online mode. Finally, the simulation results are obtained for different test cases in both the offline and the online mode. The results in the offline mode show the narrow gap between the lower and the upper bound. Moreover, the online mode indicates that the proposed method is sufficiently close to the theoretical optimal solution (the PF approach), as well as the superiority over the myopic approach, in terms of costs and rejected demands.

REFERENCES

[1] *Plug-In Electric Vehicles Sales*. Accessed: Jul. 18, 2019. [Online]. Available: https://www.energy.gov/eere/vehicles/articles/fotw-1057-november-26–2018-one-million-plug-vehicles-have-been-sold-united

[2] Q. Wang, X. Liu, J. Du, and F. Kong, "Smart charging for electric vehicles: A survey from the algorithmic perspective," *IEEE Commun. Surveys Tuts.*, vol. 18, no. 2, pp. 1500–1517, Jun. 2016.

[3] W. Shuai, P. Maillé, and A. Pelov, "Charging electric vehicles in the smart city: A survey of economy-driven approaches," *IEEE Trans. Intell. Transp. Syst.*, vol. 17, no. 8, pp. 2089–2106, Aug. 2016.

[4] M. Tabari and A. Yazdani, "An energy management strategy for a DC distribution system for power system integration of plug-in electric vehicles," *IEEE Trans. Smart Grid*, vol. 7, no. 2, pp. 659–668, Mar. 2016.

[5] W. Jiang and Y. Zhen, "A real-time EV charging scheduling for parking lots with PV system and energy store system," *IEEE Access*, vol. 7, pp. 86184–86193, 2019.

[6] L. Zhang and Y. Li, "A game-theoretic approach to optimal scheduling of parking-lot electric vehicle charging," *IEEE Trans. Veh. Technol.*, vol. 65, no. 6, pp. 4068–4078, Jun. 2016.

[7] A. Ghosh and V. Aggarwal, "Control of charging of electric vehicles through menu-based pricing," *IEEE Trans. Smart Grid*, vol. 9, no. 6, pp. 5918–5929, Nov. 2018.

[8] B. Alinia, M. H. Hajiesmaili, and N. Crespi, "Online EV charging scheduling with on-arrival commitment," *IEEE Trans. Intell. Transp. Syst.*, vol. 20, no. 12, pp. 4524–4537, Dec. 2019.

[9] N. Tucker and M. Alizadeh, "An online admission control mechanism for electric vehicles at public parking infrastructures," *IEEE Trans. Smart Grid*, vol. 11, no. 1, pp. 161–170, Jan. 2020.

[10] L. Zhang and Y. Li, "Optimal management for parking-lot electric vehicle charging by two-stage approximate dynamic programming," *IEEE Trans. Smart Grid*, vol. 8, no. 4, pp. 1722–1730, Jul. 2017.

[11] E. Akhavan-Rezai, M. F. Shaaban, E. F. El-Saadany, and F. Karray, "New EMS to incorporate smart parking lots into demand response," *IEEE Trans. Smart Grid*, vol. 9, no. 2, pp. 1376–1386, Mar. 2018.

[12] H. Zhang, Z. Hu, Z. Xu, and Y. Song, "Optimal planning of PEV charging station with single output multiple cables charging spots," *IEEE Trans. Smart Grid*, vol. 8, no. 5, pp. 2119–2128, Sep. 2017.

[13] H. Chen, Z. Hu, H. Luo, J. Qin, R. Rajagopal, and H. Zhang, "Design and planning of a multiple-charger multiple-port charging system for PEV charging station," *IEEE Trans. Smart Grid*, vol. 10, no. 1, pp. 173–183, Jan. 2019.

[14] M. Shafie-Khah *et al.*, "Optimal behavior of electric vehicle parking lots as demand response aggregation agents," *IEEE Trans. Smart Grid*, vol. 7, no. 6, pp. 2654–2665, Nov. 2016.

[15] A. S. A. Awad, M. F. Shaaban, T. H. M. El-Fouly, E. F. El-Saadany, and M. M. A. Salama, "Optimal resource allocation and charging prices for benefit maximization in smart PEV-parking lots," *IEEE Trans. Sustain. Energy*, vol. 8, no. 3, pp. 906–915, Jul. 2017.

[16] P. Pflaum, M. Alamir, and M. Y. Lamoudi, "Probabilistic energy management strategy for EV charging stations using randomized algorithms," *IEEE Trans. Control Syst. Technol.*, vol. 26, no. 3, pp. 1099–1106, May 2018.

[17] İ. Şengör, O. Erdinç, B. Yener, A. Taşcikaraoglu, and J. P. Catalão, "Optimal energy management of EV parking lots under peak load reduction based DR programs considering uncertainty," *IEEE Trans. Sustain. Energy*, vol. 10, no. 3, pp. 1034–1043, Jul. 2019.

[18] P. Carpentier, J.-P. Chancelier, V. Leclère, and F. Pacaud, "Stochastic decomposition applied to large-scale hydro valleys management," *Eur. J. Oper. Res.*, vol. 270, no. 3, pp. 1086–1098, 2018.

[19] M. N. Hjelmeland, J. Zou, A. Helseth, and S. Ahmed, "Nonconvex medium-term hydropower scheduling by stochastic dual dynamic integer programming," *IEEE Trans. Sustain. Energy*, vol. 10, no. 1, pp. 481–490, Jan. 2019.

[20] A. Bhattacharya, J. P. Kharoufeh, and B. Zeng, "Managing energy storage in microgrids: A multistage stochastic programming approach," *IEEE Trans. Smart Grid*, vol. 9, no. 1, pp. 483–496, Jan. 2018.

[21] J. Zou, S. Ahmed, and X. A. Sun, "Multistage stochastic unit commitment using stochastic dual dynamic integer programming," *IEEE Trans. Power Syst.*, vol. 34, no. 3, pp. 1814–1823, May 2019.

[22] A. J. Conejo, M. A. Plazas, R. Espinola, and A. B. Molina, "Day-ahead electricity price forecasting using the wavelet transform and ARIMA models," *IEEE Trans. Power Syst.*, vol. 20, no. 2, pp. 1035–1042, May 2005.

[23] A. Shapiro, W. Tekaya, J. P. da Costa, and M. P. Soares, "Risk neutral and risk averse stochastic dual dynamic programming method," *Eur. J. Oper. Res.*, vol. 224, no. 2, pp. 375–391, 2013.

[24] J. R. Birge and F. Louveaux, *Introduction to Stochastic Programming*. New York, NY, USA: Springer, 2011.

[25] J. R. Birge, "Decomposition and partitioning methods for multistage stochastic linear programs," *Oper. Res.*, vol. 33, no. 5, pp. 989–1007, 1985.

[26] M. V. Pereira and L. M. Pinto, "Multi-stage stochastic optimization applied to energy planning," *Math. Program.*, vol. 52, nos. 1–3, pp. 359–375, 1991.

[27] A. Shapiro, "Analysis of stochastic dual dynamic programming method," *Eur. J. Oper. Res.*, vol. 209, no. 1, pp. 63–72, 2011.

[28] M. H. Amini, P. McNamara, P. Weng, O. Karabasoglu, and Y. Xu, "Hierarchical electric vehicle charging aggregator strategy using Dantzig–Wolfe decomposition," *IEEE Des. Test*, vol. 35, no. 6, pp. 25–36, Oct. 2017.

[29] P. McNamara and S. McLoone, "Hierarchical demand response for peak minimization using Dantzig–Wolfe decomposition," *IEEE Trans. Smart Grid*, vol. 6, no. 6, pp. 2807–2815, Nov. 2015.

[30] A. Shapiro, D. Dentcheva, and A. Ruszczyński, *Lectures on Stochastic Programming: Modeling and Theory*. Philadelphia, PA, USA: SIAM, 2009.

[31] J. Zou, S. Ahmed, and X. A. Sun, "Stochastic dual dynamic integer programming," *Math. Program.*, vol. 175, pp. 1–42, Mar. 2018.

[32] V. L. De Matos, A. B. Philpott, and E. C. Finardi, "Improving the performance of stochastic dual dynamic programming," *J. Comput. Appl. Math.*, vol. 290, pp. 196–208, Dec. 2015.

[33] *Plugin Cars*. Accessed: Oct. 16, 2019. [Online]. Available: https://www.plugincars.com

[34] *EV Database*. Accessed: Oct. 16, 2019. [Online]. Available: https://ev-database.org

[35] *On-Street Car Parking Sensor Data 2016—City of Melbourne*. Accessed: Oct. 16, 2019. [Online]. Available: https://data.melbourne.vic.gov.au/Transport/On-street-Car-Parking-Sensor-Data-2016/dj7e-rdx9

[36] N. McGuckin and A. Fucci, "Summary of travel trends: 2017 national household travel survey," Nat. Res. Council, Washington, DC, USA, Rep. FHWA-PL-18-019, 2018.

[37] *Pennsylvania–New Jersey–Maryland Interconnection (PJM)*. Accessed: Nov. 25, 2016. [Online]. Available: http://www.pjm.com

[38] S. Wang, S. Bi, and Y. J. A. Zhang, "Reinforcement learning for real-time pricing and scheduling control in EV charging stations," *IEEE Trans. Ind. Informat.*, early access, Oct. 31, 2019, doi: 10.1109/TII.2019.2950809.

[39] M. Smith and J. Castellano, "Costs associated with non-residential electric vehicle supply equipment: Factors to consider in the implementation of electric vehicle charging stations," U.S. Dept. Energy, Washington, DC, USA, Rep. DOE/EE-1289, 2015.

[40] *Different Business EV Charging*. Accessed: Mar. 26, 2020. [Online]. Available: https://electrek.co/2019/08/12/kwh-pricing-ev-drivers-miss-benefits/

Omid Fallah-Mehrjardi received the B.Sc. and M.Sc. degrees in computer engineering from the University of Isfahan, Isfahan, Iran, in 2011 and 2013, respectively. He is currently pursuing the Ph.D. degree in computer engineering from the Ferdowsi University of Mashhad, Mashhad, Iran. His research interests include optimization, game theory, and reinforcement learning with applications on scheduling and energy management in smart grid, and wireless communications.

Mohammad Hossein Yaghmaee (Senior Member, IEEE) is a Full Professor with the Computer Engineering Department, Ferdowsi University of Mashhad, Mashhad, Iran. From July 2015 to September 2016, and From August 2019 to July 2020, he was with the Electrical and Computer Engineering Department, University of Toronto as a Visiting Professor. His research interests are in the smart grid, software defined networking, and Internet of Things.

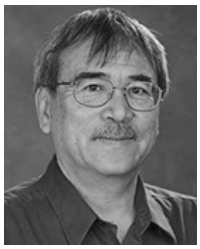

Alberto Leon-Garcia (Life Fellow, IEEE) is currently a Professor in electrical and computer engineering with the University of Toronto, Toronto, ON, Canada. He has authored the leading textbooks Probability and Random Processes for Electrical Engineering and Communication Networks: Fundamental Concepts and Key Architecture. His current research interests include application-oriented networking and autonomic resources management with a focus on enabling pervasive smart infrastructure.